CANCER

Inhibition of histone methyltransferase DOT1L silences ERα gene and blocks proliferation of antiestrogen-resistant breast cancer cells

Giovanni Nassa[1]*, Annamaria Salvati[1]*, Roberta Tarallo[1], Valerio Gigantino[1], Elena Alexandrova[1,2], Domenico Memoli[1], Assunta Sellitto[1], Francesca Rizzo[1], Donatella Malanga[3], Teresa Mirante[3], Eugenio Morelli[3], Matthias Nees[4], Malin Åkerfelt[4], Sara Kangaspeska[5†], Tuula A. Nyman[6], Luciano Milanesi[7], Giorgio Giurato[1,2‡], Alessandro Weisz[1‡]

Breast cancer (BC) resistance to endocrine therapy results from constitutively active or aberrant estrogen receptor α (ERα) signaling, and ways to block ERα pathway in these tumors are sought after. We identified the H3K79 methyltransferase DOT1L as a novel cofactor of ERα in BC cell chromatin, where the two proteins colocalize to regulate estrogen target gene transcription. DOT1L blockade reduces proliferation of hormone-responsive BC cells in vivo and in vitro, consequent to cell cycle arrest and apoptotic cell death, with widespread effects on ER-dependent gene transcription, including ERα and FOXA1 gene silencing. Antiestrogen-resistant BC cells respond to DOT1L inhibition also in mouse xenografts, with reduction in ERα levels, H3K79 methylation, and tumor growth. These results indicate that DOT1L is an exploitable epigenetic target for treatment of endocrine therapy–resistant ERα-positive BCs.

INTRODUCTION

Approximately 70% of breast tumors express estrogen receptor α (ERα), most showing hormone dependence and responding to adjuvant endocrine therapies. These therapeutic regimens target estrogen signaling in cancer cells either with synthetic ER ligands, acting as partial receptor antagonists [selective estrogen receptor modulators (SERMs)], such as 4OH-tamoxifen (TAM), and pure antagonists [selective estrogen receptor degraders (SERDs)], such as ICI 182,780 (ICI; fulvestrant), or by preventing peripheral androgen conversion to estrogen with aromatase inhibitors (*1*). Although ERα blockade is effective in the majority of cases, intrinsic or de novo resistance to endocrine therapy of receptor-positive tumors, manifesting as disease relapse or progression to a metastatic setting, represents a key problem in the clinical management of patients with breast cancer (BC). Several mechanisms have been proposed to be responsible for endocrine therapy resistance (*2*), including oncogenic activation of signaling pathways causing constitutive, ligand-independent activation of the receptor and genetic alterations of the ERα gene (*ESR1*). These include point mutations within the protein-coding sequence (*3*), in genetic elements controlling its expression (*4*) or causing functional alterations in the mitogen-activated protein kinase (MAPK) and ER pathways (*5*), that affect the ERα expression and/or protein conformation and thereby its basal- or ligand-induced activities. More recently, recurrent chromosomal aberrations causing synthesis of abnormally active ER fusion proteins have also been characterized in endocrine therapy–resistant BCs (*6*). In all these cases, it has been demonstrated that ERα signaling remains active also in the absence of estrogen and/or the presence of antiestrogens, driving gene transcription, cell proliferation, and other key cellular functions required for cell survival and tumor progression. This suggests that in these cases, down-regulation of receptor expression, or disruption of its ability to control gene transcription in cancer cells, can be more effective than estrogen deprivation. On the basis of this assumption, the molecular partners of ERα involved in the multiprotein complexes it requires for its activity on transcription, and including epigenetic regulators (*7*, *8*), represent potentially exploitable targets for new therapies against ER-positive, antiestrogen-resistant tumors.

By interaction proteomics, we identified the histone methyltransferase DOT1L (disruptor of telomeric silencing-1-like) as a component of these multiprotein complexes that assemble with ERα in BC cell nuclei after estrogen or antiestrogen treatment (*9*). DOT1L catalyzes mono-, di-, and trimethylation of histone H3 on lysine-79 (H3K79me), a marker of transcriptionally active genes, and is involved in transcription elongation, DNA repair, and cell cycle progression (*10*). This enzyme associates with mixed lineage leukemia (MLL) fusion proteins, exerting a key role in the transcriptional mechanisms sustaining leukemogenesis, and for this reason, its inhibitors have been proposed and are being clinically tested as therapeutic targets for MLL fusion leukemias (*11*, *12*). Recent studies showed the potential therapeutic usefulness of DOT1L inhibition also in neuroblastoma and ovarian and prostate cancers (*13*–*15*). Direct involvement of this enzyme in promoting the aggressive phenotype of triple-negative BC by enhancing epithelial-mesenchymal transition and a stem cell–like phenotype associating with transcriptional active c-Myc/p300 complexes has also been described (*16*).

[1]Laboratory of Molecular Medicine and Genomics, Department of Medicine, Surgery and Dentistry, "Scuola Medica Salernitana", University of Salerno, Baronissi, SA, Italy. [2]Genomix4Life Srl, University of Salerno, Baronissi, SA, Italy. [3]Department of Experimental and Clinical Medicine, University "Magna Graecia", Catanzaro (CZ), Italy. [4]Institute of Biomedicine, University of Turku, Turku, Finland. [5]Institute for Molecular Medicine, Biomedicum 2U, Helsinki, Finland. [6]Department of Immunology, Institute of Clinical Medicine, University of Oslo and Rikshospitalet Oslo, Oslo, Norway. [7]Institute of Biomedical Technologies, National Research Council, Segrate, MI, Italy.
*These authors contributed equally to this work.
†Present address: Helsinki Innovation Services Ltd., Helsinki, Finland.
‡Corresponding author. Email: aweisz@unisa.it (A.W.); ggiurato@unisa.it (G.G.)

The role and functional significance of DOT1L association with ERα in hormone-responsive, luminal-like BC cell nuclei were investigated here in detail. Results demonstrate corecruitment of both factors, in combination with other epigenetic transcriptional regulators, in a sizeable fraction of ERα cistromes of MCF-7 cell chromatin, thereby influencing transcription of genes involved in key cellular functions, including *ESR1* (encoding ERα), *FOXA1*, and those of other ERα coregulators. DOT1L blockade with different selective chemical inhibitors, including pinometostat, currently tested in clinical trials for MLL-rearranged leukemia therapy, or small interfering RNAs (siRNAs) interfered with estrogen effects on gene expression and caused growth inhibition by cell cycle arrest in G_1, followed by massive apoptotic cell death, in hormone-responsive BC cell models, including also TAM- or ICI-resistant cell lines, both in vitro and in vivo, in a xenograft mouse model. These results demonstrate that DOT1L represents a novel molecular target for epigenetic therapies against hormone-responsive and ERα-positive, endocrine therapy–resistant breast tumors.

RESULTS

DOT1L is corecruited with ERα in BC cell chromatin

DOT1L was found to physically associate with ligand-bound ERα in MCF-7 cell nuclei, a result that led us to suggest a role of this enzyme in receptor functions (*9*). This possibility is supported by the fact that both proteins are often coexpressed in breast tumors. Considering the $ERα^+$ BC gene expression datasets available in the Cancer Genome Atlas (TCGA) database, 80% of the cases showed *DOT1L* mRNA levels with *Z* score values above the first quartile (fig. S1A, upper panel), with $ERα^+$ tumors with higher DOT1L expression showing worse overall and relapse-free survival compared with the low expressing ones (fig. S1A, lower panels). For this reason, we set forth to investigate in detail the nature and function of the association between these two regulatory factors in BC cell nuclei. As shown in fig. S1 (B to E), the interaction involves a ligand-activated receptor, being observed only in the presence of 17β-estradiol (E2, 10^{-8} M; fig. S1B). DOT1L associates within the C-terminal region of ERα that comprises the ligand-binding and transactivation function 2 (AF-2) domains of the protein (fig. S1C). DOT1L does not interact with ERβ (fig. S1D), the receptor subtype exerting opposite effects with respect to ERα in BC cells, where it activates antiproliferative and oncosuppressive circuities (*17*). This result suggests that this enzyme might play a specific role in the ERα-mediated regulation of gene transcription linked to the mitogenic actions of estrogen. Chromatin immunoprecipitation coupled to protein identification and label-free quantitation by mass spectrometry (ChIP-MS) was then applied to identify additional components and cofactors of the DOT1L-ERα complex in MCF-7 cells. For this, in vivo cross-linked chromatin was fragmented and immunoprecipitated with anti-ERα, anti-DOT1L, or control antibodies and subjected to MS analysis, and the proteins copurified with each of the two factors in the genome were identified, as described in Materials and Methods. As shown in Fig. 1A (left), ERα immunoprecipitates contain also DOT1L and the receptor is present in DOT1L samples, indicating that both proteins associate together with chromatin, a result confirmed in soluble protein extracts (fig. S1E). Overall, MS analysis identified 614 nuclear proteins copurified with ERα and 570 with DOT1L, the large majority (515) in common between the two factors (Fig. 1A and table S1). As shown in fig. S2A, these protein sets comprise 94 known interactors of ERα, 45 of DOT1L and 20 of both factors. Functional annotation analysis of the 515 proteins in common between the ERα and DOT1L indicates that these are involved in multiple biological processes (Fig. 1B), reflecting known effects of estrogen in BC, such as cell death and survival, gene expression, cellular growth and proliferation, DNA replication, and cell cycle, as well as those of DOT1L in leukemia and other cancers. This list includes known transcriptional coregulators of ERα, such as GREB1, NRIP1, and SMAD3 (*18*, *19*), the bromodomain proteins BRD2 and BRD4 (*8*, *20*), KMT2A (MLL1/MLL), and KMT2D (MLL4), known to physically and functionally associate with both ERα and DOT1L (*7*, *21*). Mapping ERα and DOT1L binding to MCF-7 cell genome by ChIP sequencing (ChIP-seq) confirmed colocalization of the two proteins in a sizeable number of chromatin sites. As summarized in Fig. 1C, by comparing the positioning of the 33,492 ERα and 14,799 DOT1L binding sites identified, three main clusters emerged, representing ERα-only (red), DOT1L-only (blue), and ERα + DOT1L (green) binding sites (Fig. 1C and table S2, A to C). As reported in fig. S2B, the binding regions center in all three cases on transcription start sites (upper panels), with a larger number of ERα-only and ERα + DOT1L sites located in introns and DOT1L-only sites mainly found in intergenic regions (lower panels). ERα + DOT1L binds more often within enhancer and promoter regions, compared with ERα or DOT1L alone. A search for overrepresented transcription factor binding motifs in the binding sites identified revealed a prevalence of ERE (estrogen response element) or ERE-like sequences in ERα-only and ERα + DOT1L sites, and of FOXP1 binding matrices in DOT1L-only sites (Fig. 1C, right). Of note, FOXP1 is among the proteins found to be associated with DOT1L by ChIP-MS (table S1E). When considering that DOT1L does not bind DNA, these results suggest that its association with ERα could drive this enzyme to regulatory sites, such as enhancers and promoters, where the two proteins cooperate to regulate gene activity.

DOT1L inhibition interferes with ER-mediated transcription and causes growth arrest and death in hormone-responsive BC cells

To investigate the functional significance of the ERα-DOT1L interaction in BC cell nuclei, estrogen-stimulated cells were treated with the selective DOT1L inhibitor EPZ004777 (EPZ), which has been shown to decrease H3K79 methylation and to block expression of leukemogenic genes (*11*). As shown in Fig. 2A (left), EPZ causes a time- and concentration-dependent decrease in global mono-, di-, and trimethylated H3K79 levels in MCF-7 cell chromatin, more pronounced for the dimethylated form (H3K79me2), which after 3 days decreased by >70% (Fig. 2A, right), showing a response comparable to what was observed by Daigle *et al.* (*11*) in MLL cells under comparable experimental conditions. As H3K79 methylation by DOT1L is coupled with gene transcription (*22*), H3K79me2 ChIP-seq was then performed before and after DOT1L blockade with 6.4 μM EPZ for 6 days (Fig. 2B). Results highlight the presence of H3K79me2 only in actively transcribed genes, detected by Nascent-seq (see below), more evident in those harboring DOT1L-alone or ERα-DOT1L binding sites within or near the transcription unit (TU; central panels of Fig. 2B). Methylated histones are positioned prevalently toward the 5′ of the TUs and decrease substantially after EPZ treatment. To evaluate the relationships between transcriptional gene regulation by ERα and H3K79 methylation, MCF-7 cells were treated for 3 days with the pure antiestrogen ICI, inducing ERα down-regulation, and

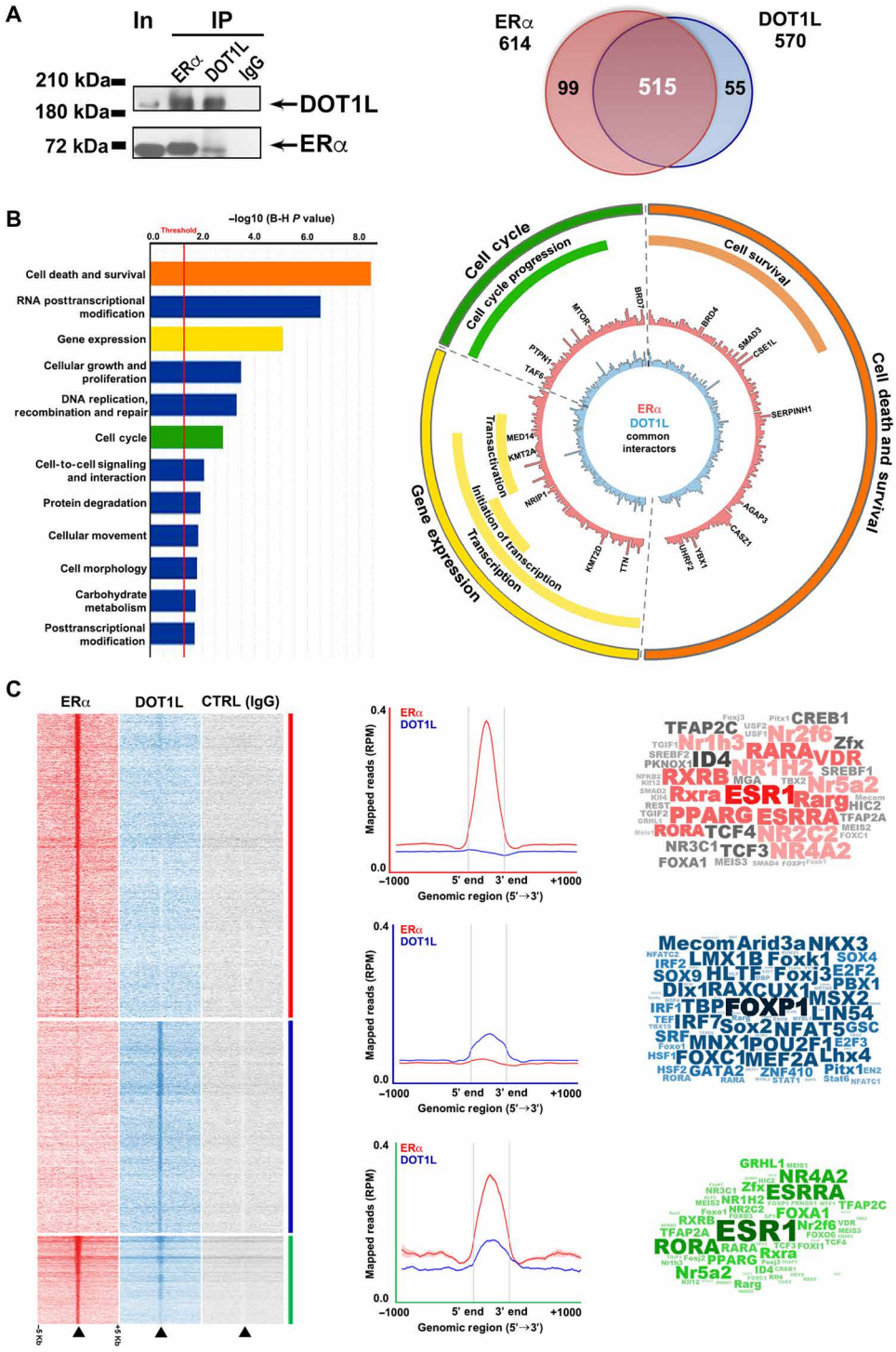

Fig. 1. Functional analysis and physical mapping of DOT1L association with ERα in MCF-7 cell chromatin. (**A**) Left: ChIP–Western blot showing DOT1L/ERα corecruitment on chromatin. Right: Venn diagram summarizing results relative to identification of a set of proteins co-associated with ERα and/or DOT1L on chromatin. (**B**) Functional enrichment analysis (left) by IPA of the protein set co-associated to both ERα and DOT1L on chromatin. In orange, yellow, and green are shown those functions where both ERα and DOT1L participate. MS-ARC (right) showing chromatin proteins co-associated with both ERα and DOT1L, clustered according to molecular functions. The ARC length is inversely proportional to Benjamini-Hochberg (B-H) corrected *P* value. Inner arches represent functional subcategories, and their overlap reveals proteins involved in different functional subcategories. Protein bar lengths indicate signal intensity within the ERα (red) and DOT1L (blue) datasets. (**C**) Left: Heat map showing read density around the 10-kb regions centered on each ERα (left) or DOT1L (center) binding sites in MCF-7 cells, with respect to control [CTRL; immunoglobulin G (IgG)]. Binding sites are clustered in the following three regions: ERα-only (red bar), DOT1L-only (blue bar), and ERα + DOT1L binding sites (green bar). Middle: Mean read densities within and around ERα-only (top), DOT1L-only (middle), and ERα-DOT1L colocalized binding sites (bottom). Right: Word cloud showing overrepresented transcription factor binding motifs within ERα-only (red, top), DOT1L-only (blue, middle), and ERα + DOT1L (green, bottom) binding sites, respectively.

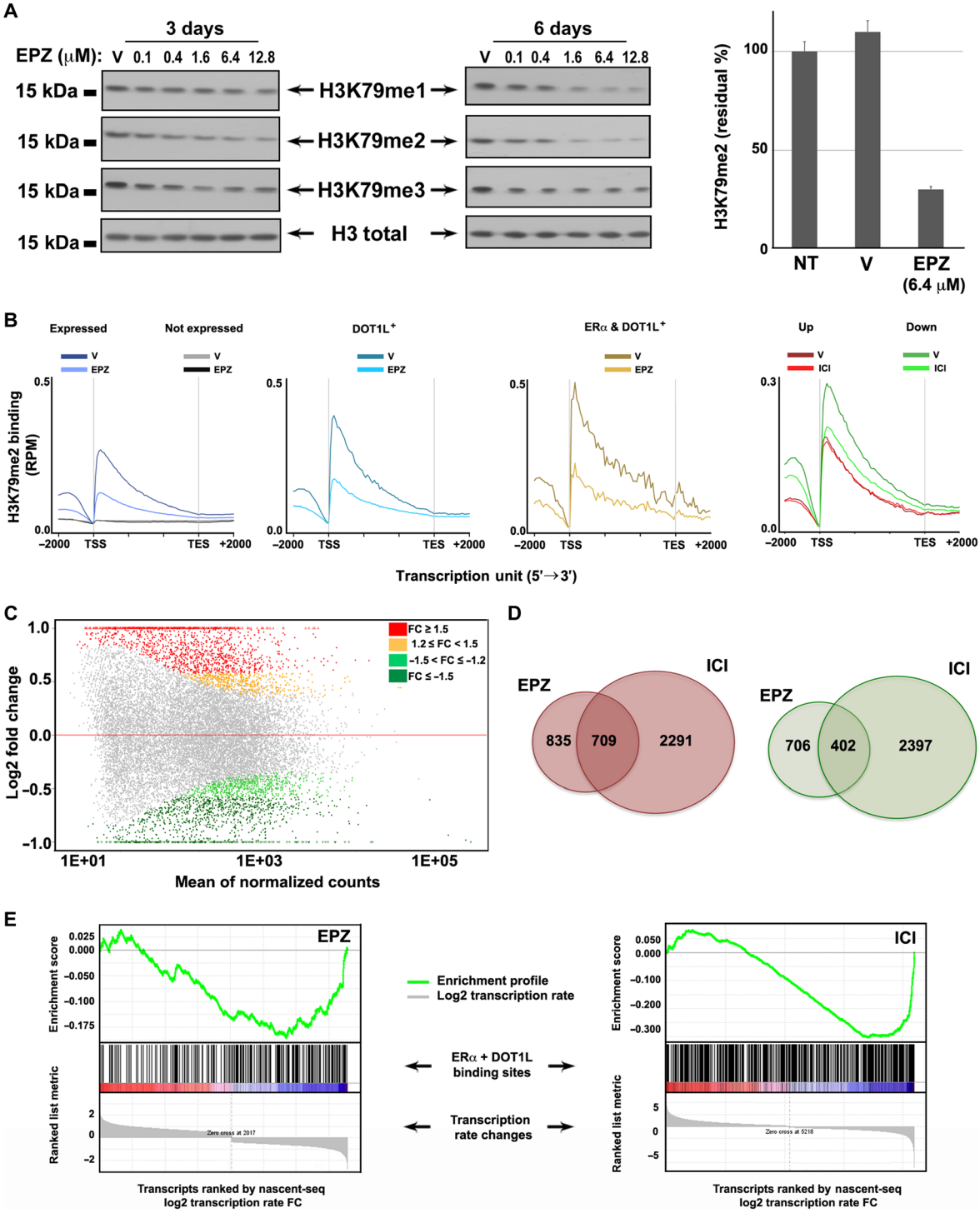

Fig. 2. DOT1L inhibition affects ERα-dependent gene transcription in MCF-7 cells. (**A**) Left: Immunoblot analysis of global H3K79me1, H3K79me2, and H3K79me3 levels in MCF-7 cells following 3 or 6 days of treatment with EPZ at the indicated concentrations. V indicates vehicle alone [dimethyl sulfoxide (DMSO), control]. Total H3 was also detected as loading control. Right: In vivo detection of H3K79me2 levels in MCF-7 cells before and after DOT1L pharmacological inhibition with EPZ (4 days). Not treated (NT) and vehicle (V) were used as controls. (**B**) ChIP-seq signal graphs tracking H3K79me2 occupancy on transcription units (TUs) without (DMSO, V) and with treatment with EPZ (6.4 μM) for 6 days. From left to right, H3K79me2 profiles in all expressed versus all not expressed TUs known, TUs harboring DOT1L alone (DOT1L$^+$) or ERα + DOT1L (ERα$^+$ and DOT1L$^+$), and activated (Up) or silenced (Down) by ERα blockade with ICI, corresponding to estrogen-repressed and estrogen-activated genes, respectively. (**C**) MA plot showing transcription rate changes [fold change (FC)], measured by nascent-seq, following 6 days of treatment with EPZ (6.4 μM). (**D**) Venn diagram showing the number of RNAs whose transcription rate is affected following 3 and 6 days of treatment with either 100 nM ICI or 6.4 μM EPZ. (**E**) Gene set enrichment analysis (GSEA) analysis of EPZ- and ICI-induced transcription rate changes in transcripts harboring ERα + DOT1L binding sites. A pronounced co-occupancy was observed in both cases proximity of down-regulated transcripts.

the effects on gene transcription rate were measured by Nascent-seq and compared with those relative to the amount of methylated H3K79 present within transcription units (TUs). As expected, blockade of ERα activity caused significant changes of transcription rate in a large number of genes (table S3C). Compared with activated ones, genes inhibited by ICI contain on average significantly higher levels of H3K79me2 that reduced upon ER blockade (Fig. 2B, right panel). Since H3K79me2 levels on ICI-activated genes are not affected by antiestrogen treatment, these results suggest a link between transcriptional gene activation by estrogen (represented by ICI-inhibited genes) and H3K79 methylation by DOT1L. This was explored in more detail by measuring changes in gene transcription rates by Nascent-seq after EPZ or ICI treatment. DOT1L inhibition by EPZ changed the transcription rate of ca. 2500 genes (Fig. 2C and table S3, A and B), including many known to be regulated directly by ERα in BC cells (*23*). On the other hand, the gene response to ICI was greater and more extended than that to EPZ (fig. S2 B and C, and table S3C). However, about one-third of the genes affected by DOT1L inhibition responded similarly to ERα blockade (709 up- and 402 down-regulated; Fig. 2D). TUs whose transcription is silenced by the two inhibitors are significantly enriched for ERα + DOT1L sites (Fig. 2E), further supporting the existence of a cooperation between the two proteins in estrogen-mediated transcriptional regulation in BC cells. This was confirmed also by functional evaluation of whole transcriptome changes induced in these cells by EPZ, which showed, among the pathways most affected by DOT1L blockade, inhibition of estrogen signaling, cell cycle, and DNA replication and activation of p53, transforming growth factor–β, PI3K (phosphatidylinositol 3-kinase)–AKT, and apoptosis signaling (Fig. 3A and table S4, A and B).

Demonstrating that DOT1L plays an active part in the mitogenic and cell survival effects of estrogen in BC cells raises the possibility that this enzyme could represent a potential target to inhibit cancer cell addiction to estrogen, in analogy with the use proposed for its inhibitors in MLL-rearranged leukemias and other tumors. The effects of EPZ on MCF-7 cell proliferation was thus evaluated in detail, and results showed that it causes a dose-dependent inhibition of cell growth that, at concentrations between 6.4 and 12.8 μM, was comparable to that caused by TAM or ICI (Fig. 3B). This effect results from a block of cell cycle progression in G_1 (Fig. 3C) and massive induction of apoptotic cell death (Fig. 3, D to F), similar to what was induced by ICI, although with slower kinetics. Growth and survival of these luminal-like BC cell lines are strictly dependent on estrogen, as confirmed here by the growth arrest and cell death caused by the inhibition of estrogen signaling with TAM or ICI (left panel of Fig. 3B). The growth inhibitory effects of EPZ could thus be the consequence of an interference with estrogen actions in these cells. To investigate this possibility, the effects of EPZ were tested also in hormone-starved cells stimulated with a mitogenic dose of E2. Results showed that the drug was highly effective also in this experimental setting, where at a concentration of 6.4 μM, it caused inhibition of estrogen-induced cell proliferation by G_1 arrest and apoptotic cell death (Fig. 3G). These results suggest a link between ERα and DOT1L activities, which was further suggested by the finding that EPZ interfered to a similar extent with the transactivating functions of ERα on an ERE-luc reporter gene stably integrated in MCF-7 cells (Fig. 3H) and that inhibition of cell proliferation was observed also in other $ERα^+$, estrogen-responsive BC cell lines (BT-474, T47-D, ZR-75.1, and ZR-75.30) under both the experimental conditions described above (fig. S3). Under the same experimental conditions, no significant response was observed, instead, in ERα-, hormone-unresponsive MDA-MB-231, although in the presence of H3K79me inhibition (fig. S4A), nor in HCC 1806, Hs 578T, and MDA-MB-468 cells (fig. S4B). The results obtained here in MDA-MB-231 cells are in contrast with what was reported by Zhang and colleagues (*24*), where an effect of DOT1L inhibitors on the proliferation of these cells was observed instead, which may be due to differences in experimental settings, since DOT1L blockade has been shown to have an effect on BC stem cell proliferation and survival (*16*), which may ultimately result also in the reduction in cell number.

Three-dimensional (3D) cell cultures embedded in the extracellular matrix better recapitulate the complex architecture of human tumors, with respect to 2D cultures, promoting formation of organotypic acinar structures or spheroids (organoids) with physiologically relevant cell-cell and cell-matrix interactions, epithelial polarization, and differentiation, recapitulating human cancer histology in vivo (*25*). The effects of EPZ on cell morphology, polarization, and growth were thus evaluated also in 3D MCF-7 cell cultures, as described in Materials and Methods. EPZ induced significant effects in key morphofunctional parameters of MCF-7 cell organoids (fig. S5, A to C), including blockade of growth (area), more pronounced at day 9 of treatment, matched by increased cell death (density red) and accompanied by structural changes, represented by loss of their original shape (roundness) and characteristic of epithelial or acinar differentiation, and decrease in the length of "appendages" (max appendage), protrusions from the organoid mimicking invasiveness. The same effects were observed in ZR75.1, but not in MDA-MB-468 cells (fig. S5, D and E), confirming what was obtained in 2D cultures (fig. S5B). Together, these results demonstrate that DOT1L blockade affects ER^+ BC cell proliferation, survival, and, possibly, aggressiveness, confirming the results obtained in 2D culture models and further supporting the existence of a functional link between ERα and DOT1L to control key phenotypes of hormone-responsive BC cells.

DOT1L activity is required for efficient estrogen signaling in BC cells

The overlap between the effects of DOT1L blockade on gene transcription with those elicited by antiestrogens indicates that this enzyme is involved in the control of key steps of the estrogen pathway in MCF-7 cells. Searching for one or more genomic targets of DOT1L endowed with a "master" role in estrogenic signaling, we implemented the IPA Upstream Regulator analysis. This method exploits the known effects of master upstream regulatory factors (URs) on their target genes to pinpoint key regulators responsible for the global gene expression changes detected in response to a given stimulus or condition. It takes into account the number of transcripts encoded by known target genes of transcriptional regulators and, for each of these, the direction of change with respect to the control (i.e., increase or decrease). This method was implemented on transcriptomics data from MCF-7 cells treated with EPZ, TAM, or ICI [tables S3 (A and B), S4 (A and B), and S5A] and ZR-75.1 cells treated with EPZ (table S5B), searching for evidence of URs whose activity was similarly affected by the two antiestrogens and EPZ. Results highlighted 45 factors affected in the same way (activation or inhibition) in all cases (Fig. 4A). ESR1 was the top hit among inhibited URs, together with its pioneering factor FOXA1 (*26*) and coregulators GATA3 (*27*) and CTR9 (*28*). This result was confirmed experimentally, since EPZ treatment decreased ERα mRNA and protein levels in a time- and dose-dependent

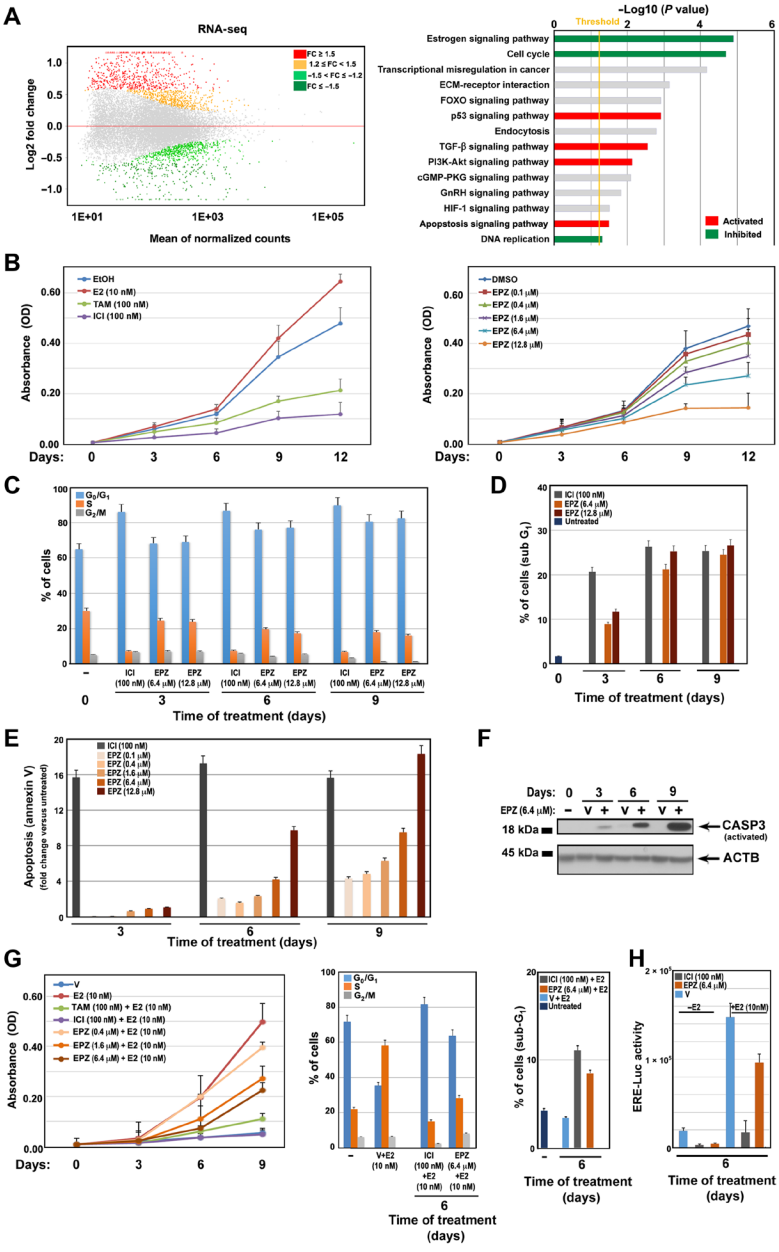

Fig. 3. Pharmacological inhibition of DOT1L affects gene expression and key cellular functions, including proliferation and survival, in MCF-7 cells. (**A**) Left: MA plot showing transcriptome changes, measured by RNA sequencing (RNA-seq), following 6 days of treatment with 6.4 μM EPZ. Right: Bar chart, obtained from KEGG functional enrichment analysis, showing statistically significant deregulated pathways. Green, red, and gray colors represent inhibited, activated, and unaffected signaling pathways, respectively. (**B**) MCF-7 cell proliferation rate in the presence of estrogen (17β-estradiol, E2), the indicated antiestrogens, or increasing concentrations of EPZ, assessed by MTT assays in exponentially growing conditions. Vehicles (EtOH or DMSO) were used as controls. (**C** and **D**) Cell cycle phase distribution in exponentially growing MCF-7 cell cultures before (–) and after treatment with the indicated concentrations of ICI or EPZ for 3 to 9 days. Percentages of G_1, S, and G_2/M (C), and sub-G_1 (D) phase cells were determined by flow cytometry after propidium iodide (PI) staining. (**E**) Bar chart showing accumulation of annexin V–fluorescein isothiocyanate (FITC)/PI–positive cells following treatment with the indicated concentrations of either ICI or EPZ for 3, 6, and 9 days. For (B) to (E), the results shown represent the means ± SD of multiple determinations from a representative experiment performed in octuplicate (B) or triplicate (C to E). (**F**) Western blot showing the extent of activated caspase-3 (CASP3) accumulation after 3, 6, or 9 days of treatment with EPZ (+, 6.4 μM) or vehicle (V, DMSO) in MCF-7 cells. β-Actin (ACTB) was used as loading control. (**G**) Left: MCF-7 cell proliferation rate in the presence of estrogen only (17β-estradiol, E2), the indicated antiestrogens, or increasing concentrations of EPZ with E2 coadministration, assessed by MTT assays in hormone-starved cells. Vehicle (EtOH) was used as control. Middle and right: Cell cycle phase distribution in hormone-deprived MCF-7 cell cultures before (–), after E2 only, or treatment with the indicated concentrations of ICI or EPZ for 6 days together with E2. Percentages of G_1, S, and G_2/M (middle), and sub-G_1 (right) phase cells were determined by flow cytometry after PI staining. Results shown represent the means ± SD of multiple determinations from a representative experiment performed at least in triplicate. (**H**) ERα transactivating activity in MCF-7 cells stably expressing the ERE-Luc reporter gene (MELN), before and after E2 stimulation, in the presence of either vehicle only (V) or the indicated concentrations of ICI or EPZ. Results shown represent the means ± SD of multiple determinations from a representative experiment performed in triplicate. OD, optical density.

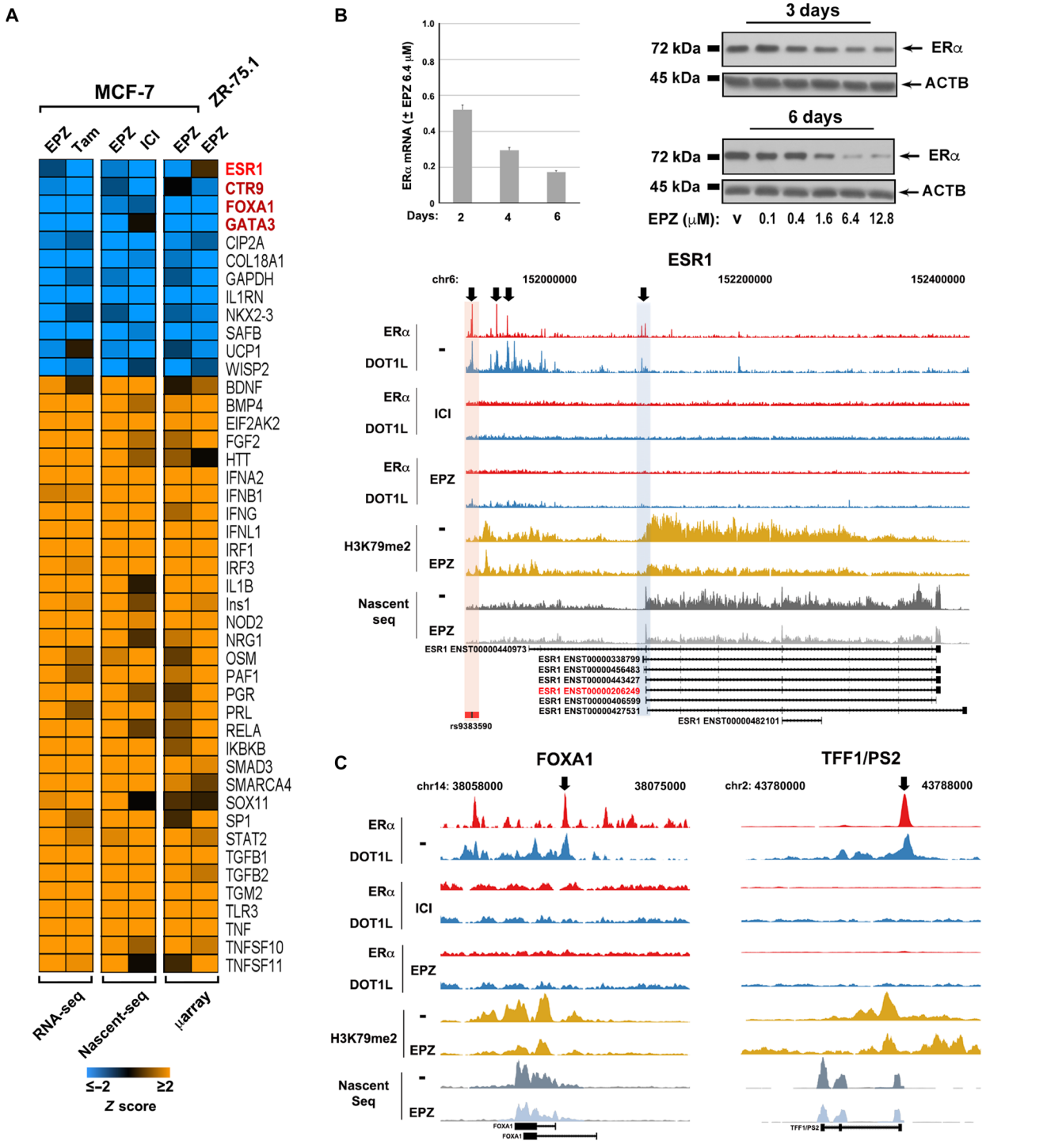

Fig. 4. ER-DOT1L interaction is required for ERα expression and signaling. (**A**) Heat map showing results of Upstream Regulator analysis by IPA (activation *Z* score values) in MCF-7 or ZR-75.1 cells, performed on RNA-seq, nascent-seq, or microarray gene expression profiling data from cells treated with EPZ (6.4 μM), TAM (100 nM), or ICI (100 nM). The effects (down-regulation) on ERα (ESR1) and three ERα functional partners, key regulators of estrogen-mediated transcriptional regulation, are highlighted in red. (**B**) Top: Reverse transcription quantitative real-time polymerase chain reaction (RT-qPCR) (left) and immunoblot analysis (right) showing ERα mRNA and protein levels following cell treatment with the indicated concentrations of EPZ. Treatment with vehicle alone (V, DMSO) was used as control. RT-qPCR results are shown as means ± SD of multiple determinations from a representative experiment. β-Actin (ACTB) was used as loading control for immunoblots. Bottom: Screenshot of ESR1 locus, depicting ERα (red) and DOT1L (blue) ChIP-seq signals before and after EPZ (6.4 μM) for 6 days or ICI (100 nM) for 3 days, together with H3K79me2 ChIP-seq (yellow) and nascent-seq (gray) data before and after EPZ. Arrows indicate ERα + DOT1L binding sites, and the red/blue strips highlight relevant enhancer and the promoter regions. The ESR1 isoform reported in red resulted in the most abundant one from RNA-seq experiments. (**C**) Screenshots of FOXA1 and TFF1/PS2 loci showing ERα, DOT1L, and H3K79me2 ChIP-seq data following the same scheme described above.

manner (>80% after 6 to 8 days; Fig. 4B). ChIP-seq data provided mechanistic evidence to explain the effects of the drug on *ESR1* silencing, as DOT1L was found to be associated with key regulatory sites of the gene, in the promoter region and an upstream enhancer, tethered to ERα (Fig. 4B). Both EPZ and ICI caused complete loss of ERα and DOT1L binding to these sites, accompanied by notable reduction in H3K79me2 levels along the TU, accumulation of H3K9me3 and H3K27me3 and decrease in H3K4me3 on the promoter (fig. S6A), epigenetic marks of gene repression in the former and activation in the latter, and *ESR1* transcription rate (Fig. 4B). Several other known estrogen-responsive genes, including in particular *FOXA1* and *TFF1* (Fig. 4C), showed a similar response to the inhibitors. The upstream *ESR1* enhancer is of particular interest, as it is known to physically interact with the promoter to regulate its activity and includes the single-nucleotide variant rs9383590, which has been shown to promote sustained ESR1 expression in BC and to be associated with enhanced BC risk (*4*). Enhancer regions often transcribe small noncoding RNA, named "enhancer RNAs" (eRNAs), involved in enhancer-promoter looping and thereby regulation of the target gene (*29*). Changes in enhancer activity are often accompanied by changes in the expression of their eRNAs, whose levels are therefore markers of enhancer activity. EPZ treatment affected eRNAs of 372 enhancers in MCF-7 cells (table S6) and, among these, decreased *ESR1* enhancer eRNAs (fig. S6), demonstrating reduced activity of this genetic element upon DOT1L blockade. These results were further supported by the fact that ERα reduction induced by either EPZ or ICI results in a mirroring reduction in DOT1L on the common chromatin binding sites (fig. S6B), including in particular both enhancer and promoter sites located upstream of the ESR1 gene (fig. S6C). Effects comparable to those of EPZ were observed with other small-molecule DOT1L inhibitors, in particular EPZ-5676 (pinometostat) (*12*), currently in clinical trials for use against MLL-rearranged acute leukemia (*30*, *31*), and the EPZ-brominated analog SGC0946 (*32*). Both these compounds were highly effective in reducing H3K79me1, H3K79me2, and H3K79me3 and ERα mRNA and protein levels in MCF-7 cells (fig. S7A), and in strongly inhibiting MCF-7 and ZR-75.1, but again, not MDA-MB-231, cell proliferation (fig. S7B). The effects of the three different DOT1L inhibitors on ERα expression and MCF-7 cell proliferation were mimicked by siRNA-mediated knockdown of the enzyme (fig. S8, A to C), which, as expected, affected also *TFF1*, *GATA3*, and *FOXA1* (fig. S8D).

Last, the effects of DOT1L blockade by either EPZ or siRNA-mediated silencing were assessed in MCF-7 cells on the set of early estrogen-responsive genes identified here by Cirillo *et al.* (*9*). As shown in fig. S8 (D and E), results revealed that the majority of these were affected in the same way by the two treatments, consisting in a blockade of the effect of the hormone, with a significant overlap between the two sets.

Together, these results point to DOT1L as a key mediator of ERα signaling in BC cells, acting as an epigenomic transcriptional cofactor of the receptor that contributes also to maintain optimal *ESR1* gene activity.

EPZ inhibits growth of antiestrogen-resistant BC cells in vitro and in a xenograft mouse model in vivo

The results reported above demonstrate a dual role for DOT1L on ERα signaling in hormone-responsive BC cells, the first by its physical and functional association with the receptor, which is required for efficient regulation of gene transcription in response to hormone stimulation, and the second by sustaining expression of ERα and other key components of its signaling pathway, by promoting direct transcription of the corresponding genes. This evidence suggests that this enzyme could represent an ideal drug target to silence the ERα pathway in endocrine therapy–resistant breast tumors that maintain hormone responsiveness and express mutated and/or constitutively active receptor (*2*–*4*, *6*). We therefore tested the effects of EPZ in LCC2 cells, a well-characterized TAM-resistant BC cell model (*33*). As shown in Fig. 5, LCC2 expresses ERα and DOT1L, the former at a slightly lower level compared with MCF-7 (Fig. 5A), and their growth rate was stimulated by E2 and inhibited by ICI, but not by TAM (Fig. 5B). Global analysis of gene expression in response to TAM confirmed lack of significant gene responses in LCC2 (fig. S9, A and B, and table S7A). The association between ERα and DOT1L was detectable also in this cell line by coimmunoprecipitation, despite the lower ERα protein level (fig. S10A). Upon exposure to EPZ, these cells showed, instead, a marked inhibition of growth (Fig. 5B), H3K79 methylation (fig. S10B), and cell cycle progression (Fig. 5C), accompanied by increased apoptosis (Fig. 5D and fig. S10C) and decreased ERα mRNA and protein levels (Fig. 5, E and F), and an extensive transcriptome reprogramming (table S7B). LCC2 responses to DOT1L inhibition was comparable with those induced by ICI (Fig. 5, B to D) and, most importantly, by EPZ in wild-type (wt) MCF-7 cells (Fig. 3). Comparative transcriptome analysis of LCC2 versus MCF-7 cells treated with EPZ showed a remarkable number of similar gene responses, including inhibition of *ESR1*, *FOXA1*, and *GATA3* gene expression (fig. S9C), confirming the results obtained by DOT1L silencing and reflected by similar results of the IPA Upstream Regulator analysis, which yielded the same UR factor responses in both cell lines, including, in particular, inhibition of ESR1, CTR9, FOXA1, and GATA3 signaling (fig. S9D). The antiproliferative effects of EPZ were observed also in several other hormone-responsive and TAM-resistant BC cell lines, recently isolated by Kangaspeska *et al.* (*34*), including MCF-7–Tam1, BT-474–Tam1 and BT-474–Tam2, ZR-75.1–Tam1 and ZR-75.1–Tam2, and T-47D–Tam1 and T-47D–Tam2 cells (fig. S10, L to O).

Unlike TAM, ICI is a pure antagonist, preventing receptor dimerization and trans-acting functions by competing for endogenous hormone binding and leading to ERα degradation (*1*). ICI acts in a specific way, compared with TAM, and BC resistance to the two drugs results from different mechanism(s) (*2*). 182^{R}-6 is an ICI-resistant BC cell line derived from MCF-7/S0.5 (S0.5), isolated from MCF-7 cells by gradual adaptation to low serum (*35*). Both S0.5 and 182^{R}-6 cells show much lower ERα expression, compared with MCF-7, which impeded association validation by coimmunoprecipitation (Fig. 5G and data not shown), and are growth inhibited by TAM (Fig. 5H and fig. S10E). Treatment with EPZ inhibited ER expression and H3K79 methylation (Fig. 5, M and N, and fig. S10, D, F, and H) in both cell lines, accompanied by substantial growth inhibition, to an extent comparable to that induced by TAM (Fig. 5H and fig. S10E), consequent to G_1 arrest and apoptosis (Fig. 5, I to L, and fig. S10, G and I). These results indicate that blockade by DOT1L inhibition of ERα expression and, as a consequence, activity causes growth arrest, accompanied by massive apoptotic cell death, and interferes with the hormonal pathway in antiestrogen-resistant, $ERα^{+}$ BC cells independently from the cellular background and the molecular mechanism responsible for resistance to the drug.

Given the practical implications of these findings for cancer therapy, they were challenged in an animal model of TAM-resistant $ERα^{+}$

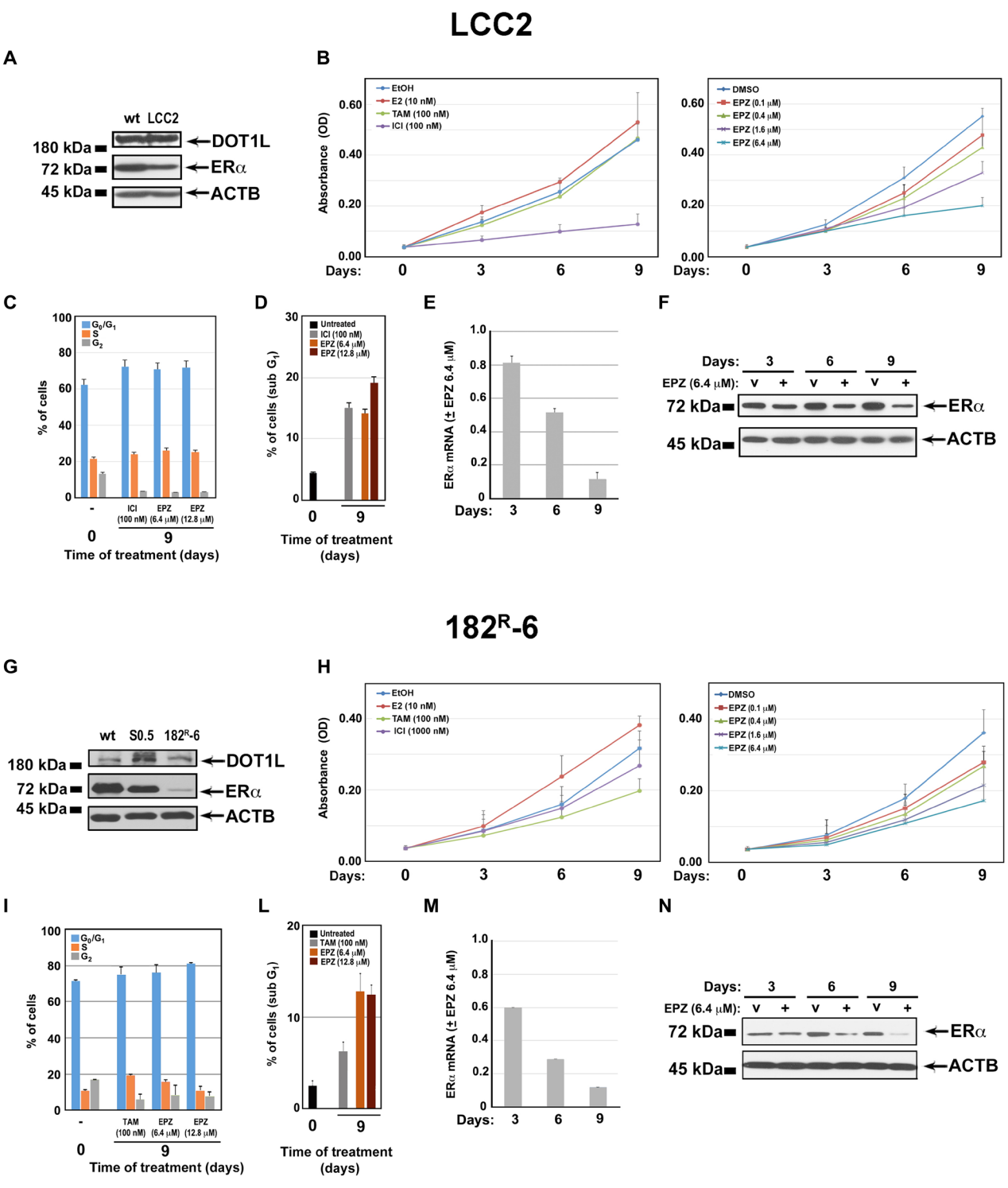

Fig. 5. DOT1L blockade inhibits SERM- and SERD-resistant BC cell proliferation. (**A** and **G**) Western blots showing ERα and DOT1L protein levels in SERM (TAM)–resistant LCC2 and SERD (ICI 182,780)–resistant MCF-7/182^R-6 cells, compared with the same in antiestrogen-sensitive (wt and S05) MCF-7 cells. (**B** and **H**) Cell proliferation rate in the presence of estrogen (17β-estradiol, E2) and the indicated antiestrogens (left) or increasing concentrations of EPZ (right) in exponentially growing cells, assessed by MTT assay. Vehicles (EtOH or DMSO) were used as controls. Results shown are the means ± SD of octuplicate determinations from a representative experiment. (**C** and **D** and **I** to **L**) Cell cycle phase distribution in cell cultures before (–) and after treatment with the indicated concentrations of ICI, TAM, or EPZ for 9 days. Percentages of G_1, S, and G_2/M (C and I), and sub-G_1 (D and L) phase cells were determined by flow cytometry after PI staining. (**E**, **F**, **M**, and **N**) RT-qPCR (left) and immunoblot analysis (right) showing ERα mRNA and protein levels following cell treatment with EPZ for the indicated times. Treatment with vehicle alone (V, DMSO) was used as control. RT-qPCR results are shown as means ± SD of multiple determinations from a representative experiment. β-Actin (ACTB) was used as loading control for immunoblots.

BC to assess whether EPZ was capable of inhibiting tumor growth also in vivo. To this aim, orthotopic xenograft models were established by injecting luciferase-expressing MCF-7–Luc or LCC2-Luc cells in the mammary fat pad of nonobese diabetic (NOD)/severe combined immunodeficient (SCID) mice, and tumor size was monitored by weekly measurement of bioluminescence signals. At 21 to 28 days from cell inoculation, when tumor sizes reached 50 to 150 mm^3, mice were randomized into treatment and control groups (eight per group) and implanted with mini-osmotic pumps loaded with EPZ (50 mg/ml) or vehicle alone, as described in Materials and Methods. This dose has been shown sufficient to achieve average EPZ circulating levels of 0.55 ± 0.12 μM (*12*), lower than the concentration causing maximum inhibitory effects in BC cells in vitro but sufficient to achieve a partial response to this drug in MLL cells in vivo, under comparable conditions (*11*). Tumor growth was then monitored at 7, 14, and 21 days, when all animals were euthanized and tumors were harvested and analyzed for H3K79me2 and ERα levels. MCF-7 and LCC2 tumors in mice treated with EPZ showed five- and threefold reduction in bioluminescence activity, respectively, compared with control (vehicle) animals, a result confirmed by measuring their weight postmortem (Fig. 6, A and B, upper panels). Immunoblot analysis of global H3K79me2 levels showed a marked reduction in EPZ versus vehicle tumors in both cases, parallel to a decrease in ERα protein levels (Fig. 6, A and B, lower panels). These data are all consistent with those described above for EPZ-treated MCF-7 cells in 2D or 3D cell models and further suggest that this enzyme represents a new, readily exploitable therapeutic target against hormone-responsive and endocrine therapy–resistant cancers.

DISCUSSION

Endocrine therapy is highly effective for the treatment of ERα-positive BCs and represents the therapeutic cornerstone to fight these diseases. Despite its proven efficacy, intrinsic and acquired resistance, manifesting clinically as a relapse or progression of the disease, occurs in ca. one-third of the cases and represents a limit to its usefulness. Among the multiple mechanisms proposed as responsible for endocrine resistance in BCs, deregulation or mutations of key components of the estrogen signaling pathway, including ERα itself, that makes it constitutive or unresponsive to hormonal antagonists have been shown to be responsible for a large fraction of these cases. For this reason, the possibility of silencing ERα expression and/or activity in cancer cells is considered an effective approach to overcome resistance in these cases. Much attention is thus being currently given to the existence of molecular components of the ER effector pathway, in particular epigenetic effectors of its nuclear pathway that can be used as novel drug targets to this end. The molecular mechanisms by which ERα promotes BC growth and progression involve formation in the cell nucleus of multiprotein complexes endowed with key functional regulatory roles (*9*, *36*, *37*). These include the coordinated assembly on chromatin of transcriptional regulatory complexes, catalyzed and targeted to specific sites by the receptor (*38*), that are responsible for conveying hormonal signaling to the genome. Several proteins that serve as epigenetic modifiers are known to be part of these complexes, and their recruitment allows the chromatin modification/remodeling steps essential to allow ERα-dependent gene regulation (*7*, *8*, *39*). We demonstrate here that the epigenetic "writer" DOT1L is guided to several regulatory sites on the genome by tethering to the receptor, including elements that control the activity of the gene encoding ERα itself and key components of its signaling pathway. The ability of DOT1L to promote transcription elongation, DNA repair, and cell cycle progression via H3K79 methylation (*10*) is essential to allow estrogen-induced promotion of BC cell proliferation and survival mediated by ERα. Inhibition of this enzyme induces a specific reprogramming of the hormone-responsive BC cell transcriptome, determining severe functional consequences in the cell, leading to cell cycle arrest and apoptotic death. Investigating the composition of chromatin-bound ERα-DOT1L interactome revealed that several of its components are already known to affect key processes in BC cells, including cell cycle progression, cell survival, and transcription, further supporting the relevance of the molecular machinery discovered here for BC cell regulation. These include, among others, known ERα interactors (*37*, *38*) as well as epigenetic regulators such as KMT2A, KMT2D, BRD2, and BRD4, and transcription regulators such as ASH2L (*40*), NRIP1 (*41*), and YBX1 (*42*), all known to be involved in the control of gene regulation by estrogen in these cells by acting in concert with ERα. The finding that an ERα-DOT1L complex binds in regulatory sites and thereby controls transcription of genes essential for hormonal signaling, including not only ERα itself but also, among others, the pioneering factor FOXA1, a key player in estrogen regulation of genome activity (*26*), revealed that this complex belongs to a positive regulatory loop maintaining optimal cellular levels of receptor and several of its functional partners. As a consequence, inhibiting the activity of this epienzyme disrupts estrogen signaling not only directly, by interference with trans-acting functions of the receptor and other transcription factors participating to the pathway (*23*), whose consensus matrices are overrepresented in the DOT1L binding sites mapped here, but also indirectly, by reducing the cellular levels of ERα and other key components of its pathway. We show here that ERα and DOT1L colocalize within the promoter and enhancer regions of the ESR1 gene and that DOT1L and the H3K79 dimethylation it catalyzes are required for ESR1 transcription. Together with FOXA1 and the other known ER interactors cited above, TRIM24, a "reader" of dual histone marks acting on estrogen-dependent genes associated with cellular proliferation and tumor development and linked to poor prognosis of BC (*43*), the progesterone receptor, recently shown to modulate ERα actions in hormone-responsive tumors (*44*), and GPER1, mediating nongenomic actions of estrogen and considered an initiator of TAM resistance in BC (*45*), are worth mentioning.

As a consequence of the positive role of DOT1L in estrogen signaling and maintenance of cellular ERα levels, its inhibition mimics the effects of antiestrogens (both SERMs and SERDs) on the cell transcriptome and behavior, in particular proliferation and ability to survive, and this might occur also by affecting BC stem cell–like properties, as demonstrated by Cho *et al.* (*16*). These results suggested that DOT1L inhibition could be exploited to induce "antiestrogen-like" responses in tumor cells that acquired resistance to these drugs during hormonal therapies. By analyzing data relative to $ERα^+$ tumors present in TCGA, we observed that aggressive tumors, with a worse prognosis that almost invariably reflects in these cases resistance to endocrine therapy, show higher DOT1L expression, further supporting the clinical relevance and usefulness of targeting this enzyme in such tumors. This possibility was challenged here on several antiestrogen (both TAM and ICI)–resistant human BC cell models, and the results obtained both in vitro and in vivo confirm

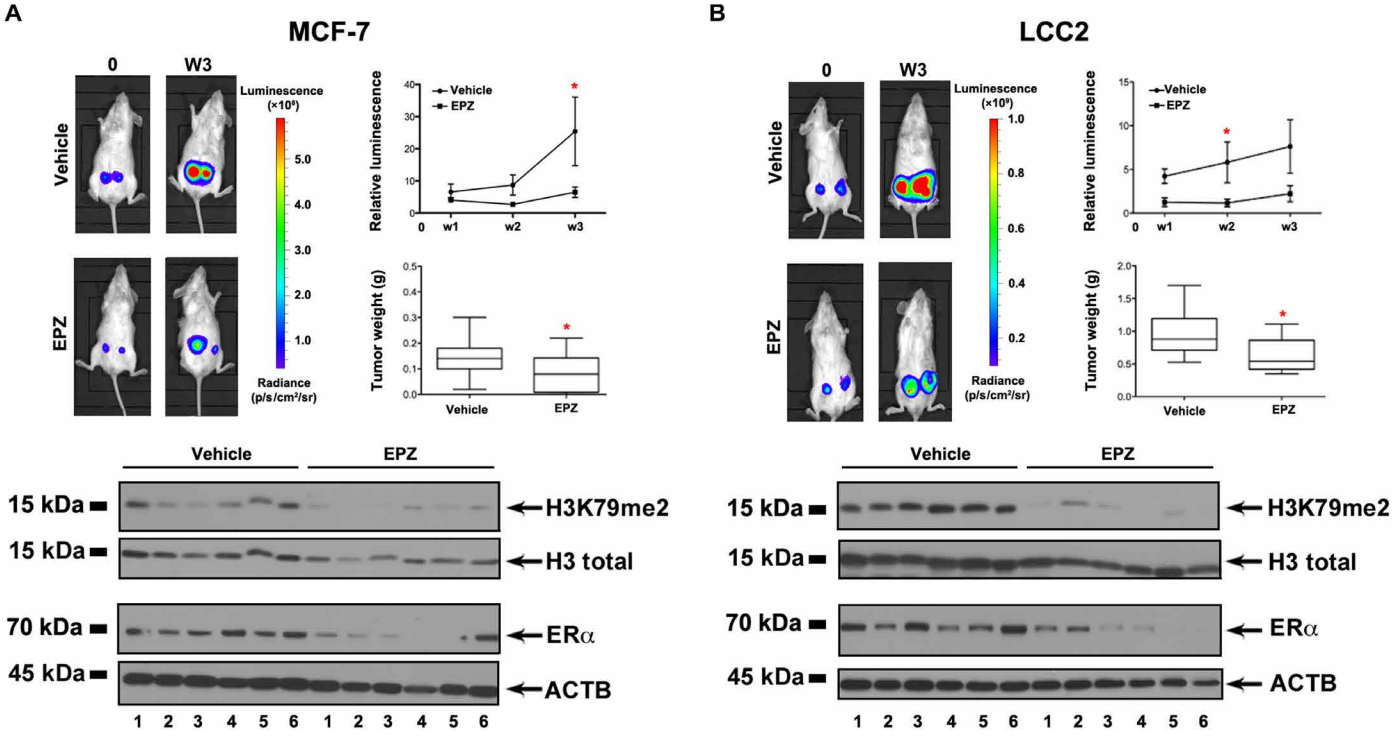

Fig. 6. DOT1L pharmacological targeting affects antiestrogen-sensitive and antiestrogen-resistant BC cell tumor progression in vivo. Top: Mice carrying tumors obtained by orthotopical injections of MCF-7–luciferase (**A**) or MCF-7/LCC2–luciferase (**B**) cells in the mammary fat pad were implanted with pumps containing either a solution of EPZ (50 mg/ml) or vehicle (DMSO). Tumor progression was assessed by bioluminescence before (0) and after 2 (W2) and 3 (W3) weeks of treatment. Representative images at 0 and W3 are shown in each case to the left, the average bioluminescence for all mice in the upper-right panels, and the final tumor volumes in the lower-right panels. The *P* values were calculated using unpaired two-sample *t* test (*$P < 0.05$). Bottom: Immunoblot analysis of H3K79me2 and ERα protein levels in tumors derived from animals treated with vehicle alone (DMSO, vehicle) or EPZ for 3 weeks. Total H3 and β-actin were used as loading controls.

that targeting DOT1L to achieve inhibition of estrogen signaling, growth inhibition, and cell death represents an actionable option against ab initio or acquired endocrine therapy resistance in BCs. Razavi *et al.* (*5*) recently showed in a large cohort of ERα$^+$ BC samples that hormone resistance arising after hormonal therapy is characterized by accumulation of mutations of *ESR1* or other genes of the receptor pathway in the tumor in ca. 20% of the cases and that mutations in these genes are significantly more common in metastases compared with primary tumors. Enrichment in these mutations was found mutually exclusive with regard to MAPK pathway genes (22% of the cases). Since the large majority of these ESR1 mutations affect receptor activity and responsiveness to ligands and the MAPK pathway activation is well known to cause phosphorylation of ERα, which thereby becomes constitutively active and insensitive to antiestrogens, it is not unexpected that in all cases, the patient fails to respond to endocrine therapy. The presence of a receptor abnormally active as a result of a structural variation caused by a mutation, or of posttranslational modifications induced by a deregulated signaling pathway, drives tumor progression with the same molecular mechanisms normally set in motion by estrogen, but insensitive to either agonist (estrogen hormones) or antagonist (TAM, ICI, etc.) ligands. In all these cases, representing a large fraction of endocrine therapy–resistant tumors, the possibility of silencing the ESR1 gene, clearing ERα from the cell, is a rational approach worth considering. DOT1L is particularly suitable to this aim, since several effective inhibitors of this enzyme are being actively investigated as potential anticancer drugs. A phase 1 clinical trial with the DOT1L inhibitor EPZ5676 used here in patients with MLL fusion gene–driven leukemia, for example, has recently ended, and the results confirmed the therapeutic potential of this approach (*30*), although its efficacy as a single agent was modest. In this respect, we observed that cotreatment of MCF-7 cells with TAM and EPZ led to an additive effect of the two drugs (data not shown), a result not surprising in view of the common downstream target of both drugs, i.e., ERα, but of interest in view of the possibility to combine DOT1L inhibitors with endocrine therapy in such cases where a more effective blockade of estrogen signaling may be beneficial. If these studies yield positive results, repositioning DOT1L inhibitors for BC therapy could benefit from a substantial reduction in the time and costs necessary to evaluate their actual efficacy against these tumors.

MATERIALS AND METHODS

Cell lines

MCF-7 (HTB-22), ZR-75.1 (CRL-1500), ZR-75.30 (CRL-150), T-47D (HTB-13), BT-474 (HTB-20), MDA-MB-231 (HTB-26), MDA-MB-468 (HTB-132), Hs 578T (HTB-126), HCC 1806 (CRL-2335), and MCF-10A (CRL-10317) were purchased from the American Type Culture Collection. TAM-resistant MCF-7/LCC2 cells (LCC2) were provided by J. Lehtio (Karolinska Institutet, Sweden). MCF-7/S0.5 (16022501) and ICI-resistant MCF-7/182^R-6 cells (16022506) were purchased from European Collection of Authenticated cell cultures. Additional details are provided in the Supplementary Materials and Methods.

Antibodies
The following antibodies were used for immunoprecipitation and Western blot analyses: C-terminal anti-ERα (sc-543, Santa Cruz Biotechnology), rabbit polyclonal anti-DOT1L (A300-953A, Bethyl Laboratories), β-actin (A1978, Sigma-Aldrich), N-terminal anti-ERα (ab75635), mouse anti-KMT4/DOT1L (ab72454), anti-histone H3 (total; ab1791), anti-H3K79me1 (ab2886), anti-H3k79me2 (ab3594), anti-H3K79me3 (ab2621), anti-H3K4me3 (ab7766), anti-H3K9me3 (ab1220), anti-H3K27me3 (ab24684) from Abcam, anti–cleaved caspase-3 (2305-PC-100, Trevigen), anti-TAP (CAB1001), and rabbit immunoglobulin G (IgG) isotype control (31235) from Thermo Fisher Scientific.

Protein extraction and coimmunoprecipitation
Total and nuclear protein extracts were prepared as described previously (*17*, *36*). Immunoprecipitation experiments have been performed in accordance with standard protocols with minor modifications. Additional details are provided in the Supplementary Materials and Methods.

Histone extraction
For histone extraction, cells were treated with DOT1L inhibitors EPZ (S7353), EPZ5676 (S7062), and SGC0946 (S7079) (all from Selleckchem) or their vehicles for 3 and/or 6 days, and the procedure was performed as described previously (*11*).

ChIP-MS and data analysis
ChIP-MS was performed as described by Mohammed *et al.* (*18*), with some modifications. Tryptic digestion liquid chromatography–MS/MS and data analysis were performed as previously described (see the Supplementary Materials and Methods for additional details) (*46*). The MS proteomics data have been deposited to the ProteomeXchange Consortium via the PRoteomics IDEntifications (*47*) partner repository with the dataset identifier PXD010314.

ChIP, sequencing, and data analysis
For ChIP-seq experiments in MCF-7 cells, antibodies against ERα, DOT1L, H3K79me2, and IgG as negative controls were used. ChIP, cell lysis, sonication, and binding were performed as previously described (*17*) using proper modifications when histone H3K79me2 was immunoprecipitated. Library preparation sequencing and data analysis were performed as described previously (*17*). The ArrayExpress accession numbers for ChIP-seq and histone–ChIP-seq data are E-MTAB-6883 and E-MTAB-6889, respectively.

Nascent RNA, total RNA, and mRNA sequencing, microarrays, and data analyses
Nascent RNA–seq, with ribosomal removal, and total RNA–seq procedures were performed as described previously (*17*). For mRNA-seq experiments, indexed libraries were prepared with the TruSeq Stranded Total mRNA Sample Prep Kit (Illumina Inc.) and sequenced according to the manufacturer's instructions. Nascent RNA–seq, total RNA–seq, and mRNA-seq data analyses were performed as described previously (*17*). Microarray experiments and data analysis were performed as described (*9*). The ArrayExpress accession numbers for nascent RNA–seq, total RNA–seq, and mRNA-seq data were E-MTAB-6871, E-MTAB-6875, and E-MTAB-6892, respectively, and E-MTAB-6893 for microarray data.

Gene set enrichment analysis
GSEA was performed as described previously (*44*).

Functional analyses
Functional analyses were performed as earlier (*17*). MS-ARC was created as described (*18*). For total RNA–seq data, pathways have been integrated with KEGG enriched pathways ($P \leq 0.05$), computed as described previously (*23*). Upstream Regulator analysis was carried out using IPA (IPA, QIAGEN Redwood City; www.qiagen.com/ingenuity).

Enhancer RNA expression analysis
Enhancer RNA expression was computed using the enhancer annotation specific for MCF-7 cells available in EnhancerAtlas (*48*). Data analysis was performed as described previously (*49*).

Cell proliferation, cell cycle, and annexin V assays
Cell proliferation assays were performed using the MTT assay (M6494, Thermo Fisher Scientific) according to the manufacturer's instructions. For cell cycle analysis, cells treated with compounds and vehicles reported in the figures and fixed in cold 70% ethanol were analyzed, as previously described (*36*), using a BD FACSVerse (BD Biosciences). Apoptosis was determined with an APC Annexin V apoptosis detection kit with PI (640932, BioLegend) according to the manufacturer's protocol. Results shown were obtained from three independent experiments. See the Supplementary Materials and Methods for details.

qPCR
See the Supplementary Materials and Methods.

DOT1L knockdown
See the Supplementary Materials and Methods.

Miniaturized organotypic 3D cultures
See the Supplementary Materials and Methods.

Xenograft experiments
Generation of luciferase expression cell lines by lentiviral transduction
MCF-7 and LCC2 cells stably expressing luciferase transgene were obtained with RediFect Red-FLuc-Puromycin Lentiviral Particles (CLS960002, PerkinElmer) according to the manufacturer's protocol. See the Supplementary Materials and Methods for details.

Xenograft experiments
NOD-SCID mice were purchased from Envigo Italy and housed at the Animal Facility of Magna Graecia University (Catanzaro, Italy). In detail, 2.0×10^6 MCF-7–Luc or LCC2-Luc cells, resuspended in 100 μl of 50:50 Matrigel/phosphate-buffered saline, were injected bilaterally into the fourth abdominal fat pad of 7-week-old female mice ($n = 8$ for each group). Mice were monitored weekly and intramuscularly injected with 200 μl of estradiol valerate oil sterile solution (10 μg/ml). Mice with xenograft tumors ranging from 50 to 150 mm^3 in size were randomized and implanted with mini-osmotic pumps loaded with a solution of EPZ (50 mg/ml) or with vehicle (15% ethanol, 50% PEG300, and 35% water), as previously described (*11*). Pumps were replaced on days 7 and 14. Tumor growth was monitored every 7 days by in vivo detection of the tumor mass using the IVIS LUMINA II Imaging System (Caliper Life sciences).

After 21 days of treatment, all mice were euthanized by CO_2 inhalation and tumors were harvested. Histone and protein extraction from xenograft are further detailed and provided in the Supplementary Materials and Methods. Animal experimentation was approved by the local ethical committee, "Organismo Preposto per il Benessere Animale," of Magna Graecia University and conformed to regulations and guidelines of Italy and the European Union (approval from the Italian Ministry of Health n264/2018-PR).

Statistical analysis

Statistical analyses were performed using R (version 3.4.4). Error bars represent means ± SD. For animal studies, statistical differences between groups were determined using unpaired two-sample *t* test. Values of $P \leq 0.05$ were considered to be statistically significant.

SUPPLEMENTARY MATERIALS

Supplementary material for this article is available at http://advances.sciencemag.org/cgi/content/full/5/2/eaav5590/DC1

Supplementary Materials and Methods
Fig. S1. ERα-DOT1L association.
Fig. S2. ERα-DOT1L functional interaction.
Fig. S3. DOT1L inhibition reduces the proliferation of ERα-positive BC cells.
Fig. S4. DOT1L inhibition in ERα-negative BC cell proliferation.
Fig. S5. DOT1L pharmacological inhibition in ERα-positive and ERα-negative 3D BC cell models.
Fig. S6. EPZ affects ESR1 activity and ERα-DOT1L binding affinity.
Fig. S7. Functional effect of alternative DOT1L inhibitors.
Fig. S8. Effects of DOT1L silencing by short hairpin RNAs on proliferation and estrogen-mediated gene expression in MCF-7 cells.
Fig. S9. Transcriptome analyses of MCF-7 and LCC2 cells following TAM treatment or DOT1L pharmacological inhibition.
Fig. S10. DOT1L pharmacological inhibition in SERM- and SERD-resistant BC cell models.
Table S1. ChIP-MS data.
Table S2. ChIP-seq data.
Table S3. Nascent-seq data in MCF-7 cells.
Table S4. RNA-seq data in MCF-7 cells.
Table S5. Microarray data in MCF-7 and ZR-75.1 cells.
Table S6. eRNA data.
Table S7. RNA-seq data in LCC2 cells.
References (*50*–*54*)

REFERENCES AND NOTES

1. K. Tryfonidis, D. Zardavas, B. S. Katzenellenbogen, M. Piccart, Endocrine treatment in breast cancer: Cure, resistance and beyond. *Cancer Treat. Rev.* **50**, 68–81 (2016).
2. C. K. Osborne, R. Schiff, Mechanisms of endocrine resistance in breast cancer. *Annu. Rev. Med.* **62**, 233–247 (2011).
3. J. A. Katzenellenbogen, C. G. Mayne, B. S. Katzenellenbogen, G. L. Greene, S. Chandarlapaty, Structural underpinnings of oestrogen receptor mutations in endocrine therapy resistance. *Nat. Rev. Cancer* **18**, 377–388 (2018).
4. S. D. Bailey, K. Desai, K. J. Kron, P. Mazrooei, N. A. Sinnott-Armstrong, A. E. Treloar, M. Dowar, K. L. Thu, D. W. Cescon, J. Silvester, S. Y. Yang, X. Wu, R. C. Pezo, B. Haibe-Kains, T. W. Mak, P. L. Bedard, T. J. Pugh, R. C. Sallari, M. Lupien, Noncoding somatic and inherited single-nucleotide variants converge to promote ESR1 expression in breast cancer. *Nat. Genet.* **48**, 1260–1266 (2016).
5. P. Razavi, M. T. Chang, G. Xu, C. Bandlamudi, D. S. Ross, N. Vasan, Y. Cai, C. M. Bielski, M. T. A. Donoghue, P. Jonsson, A. Penson, R. Shen, F. Pareja, R. Kundra, S. Middha, M. L. Cheng, A. Zehir, C. Kandoth, R. Patel, K. Huberman, L. M. Smyth, K. Jhaveri, S. Modi, T. A. Traina, C. Dang, W. Zhang, B. Weigelt, B. T. Li, M. Ladanyi, D. M. Hyman, N. Schultz, M. E. Robson, C. Hudis, E. Brogi, A. Viale, L. Norton, M. N. Dickler, M. F. Berger, C. A. Iacobuzio-Donahue, S. Chandarlapaty, M. Scaltriti, J. S. Reis-Filho, D. B. Solit, B. S. Taylor, J. Baselga, The genomic landscape of endocrine-resistant advanced breast cancers. *Cancer Cell* **34**, 427–438.e6 (2018).
6. R. J. Hartmaier, S. E. Trabucco, N. Priedigkeit, J. H. Chung, C. A. Parachoniak, P. Vanden Borre, S. Morley, M. Rosenzweig, L. M. Gay, M. E. Goldberg, J. Suh, S. M. Ali, J. Ross, B. Leyland-Jones, B. Young, C. Williams, B. Park, M. Tsai, B. Haley, J. Peguero, R. D. Callahan, I. Sachelarie, J. Cho, J. M. Atkinson, A. Bahreini, A. M. Nagle, S. L. Puhalla, R. J. Watters, Z. Erdogan-Yildirim, L. Cao, S. Oesterreich, A. Mathew, P. C. Lucas, N. E. Davidson, A. M. Brufsky, G. M. Frampton, P. J. Stephens, J. Chmielecki, A. V. Lee, Recurrent hyperactive *ESR1* fusion proteins in endocrine therapy-resistant breast cancer. *Ann. Oncol.* **29**, 872–880 (2018).
7. E. Toska, H. U. Osmanbeyoglu, P. Castel, C. Chan, R. C. Hendrickson, M. Elkabets, M. N. Dickler, M. Scaltriti, C. S. Leslie, S. A. Armstrong, J. Baselga, PI3K pathway regulates ER-dependent transcription in breast cancer through the epigenetic regulator KMT2D. *Science* **355**, 1324–1330 (2017).
8. Q. Feng, Z. Zhang, M. J. Shea, C. J. Creighton, C. Coarfa, S. G. Hilsenbeck, R. Lanz, B. He, L. Wang, X. Fu, A. Nardone, Y. Song, J. Bradner, N. Mitsiades, C. S. Mitsiades, C. K. Osborne, R. Schiff, B. W. O'Malley, An epigenomic approach to therapy for tamoxifen-resistant breast cancer. *Cell Res.* **24**, 809–819 (2014).
9. F. Cirillo, G. Nassa, R. Tarallo, C. Stellato, M. R. De Filippo, C. Ambrosino, M. Baumann, T. A. Nyman, A. Weisz, Molecular mechanisms of selective estrogen receptor modulator activity in human breast cancer cells: Identification of novel nuclear cofactors of antiestrogen–ERα complexes by interaction proteomics. *J. Proteome Res.* **12**, 421–431 (2013).
10. Z. Farooq, S. Banday, T. K. Pandita, M. Altaf, The many faces of histone H3K79 methylation. *Mutat. Res. Rev. Mutat. Res.* **768**, 46–52 (2016).
11. S. R. Daigle, E. J. Olhava, C. A. Therkelsen, C. R. Majer, C. J. Sneeringer, J. Song, L. D. Johnston, M. P. Scott, J. J. Smith, Y. Xiao, L. Jin, K. W. Kuntz, R. Chesworth, M. P. Moyer, K. M. Bernt, J. C. Tseng, A. L. Kung, S. A. Armstrong, R. A. Copeland, V. M. Richon, R. M. Pollock, Selective killing of mixed lineage leukemia cells by a potent small-molecule DOT1L inhibitor. *Cancer Cell* **20**, 53–65 (2011).
12. S. R. Daigle, E. J. Olhava, C. A. Therkelsen, A. Basavapathruni, L. Jin, P. A. Boriack-Sjodin, C. J. Allain, C. R. Klaus, A. Raimondi, M. P. Scott, N. J. Waters, R. Chesworth, M. P. Moyer, R. A. Copeland, V. M. Richon, R. M. Pollock, Potent inhibition of DOT1L as treatment of MLL-fusion leukemia. *Blood* **122**, 1017–1025 (2013).
13. L. Yang, C. Lin, C. Jin, J. C. Yang, B. Tanasa, W. Li, D. Merkurjev, K. A. Ohgi, D. Meng, J. Zhang, C. P. Evans, M. G. Rosenfeld, lncRNA-dependent mechanisms of androgen-receptor-regulated gene activation programs. *Nature* **500**, 598–602 (2013).
14. X. Zhang, D. Liu, M. Li, C. Cao, D. Wan, B. Xi, W. Li, J. Tan, J. Wang, Z. Wu, D. Ma, Q. Gao, Prognostic and therapeutic value of disruptor of telomeric silencing-1-like (DOT1L) expression in patients with ovarian cancer. *J. Hematol. Oncol.* **10**, 29 (2017).
15. M. Wong, A. E. L. Tee, G. Milazzo, J. L. Bell, R. C. Poulos, B. Atmadibrata, Y. Sun, D. Jing, N. Ho, D. Ling, P. Y. Liu, X. D. Zhang, S. Hüttelmaier, J. W. H. Wong, J. Wang, P. Polly, G. Perini, C. J. Scarlett, T. Liu, The histone methyltransferase DOT1L promotes neuroblastoma by regulating gene transcription. *Cancer Res.* **77**, 2522–2533 (2017).
16. M.-H. Cho, J.-H. Park, H.-J. Choi, M.-K. Park, H.-Y. Won, Y.-J. Park, C. H. Lee, S.-H. Oh, Y.-S. Song, H. S. Kim, Y.-H. Oh, J.-Y. Lee, G. Kong, DOT1L cooperates with the c-Myc-p300 complex to epigenetically derepress *CDH1* transcription factors in breast cancer progression. *Nat. Commun.* **6**, 7821 (2015).
17. R. Tarallo, G. Giurato, G. Bruno, M. Ravo, F. Rizzo, A. Salvati, L. Ricciardi, G. Marchese, A. Cordella, T. Rocco, V. Gigantino, B. Pierri, G. Cimmino, L. Milanesi, C. Ambrosino, T. A. Nyman, G. Nassa, A. Weisz, The nuclear receptor ERβ engages AGO2 in regulation of gene transcription, RNA splicing and RISC loading. *Genome Biol.* **18**, 189 (2017).
18. H. Mohammed, C. D'Santos, A. A. Serandour, H. R. Ali, G. D. Brown, A. Atkins, O. M. Rueda, K. A. Holmes, V. Theodorou, J. L. Robinson, W. Zwart, A. Saadi, C. S. Ross-Innes, S. F. Chin, S. Menon, J. Stingl, C. Palmieri, C. Caldas, J. S. Carroll, Endogenous purification reveals GREB1 as a key estrogen receptor regulatory factor. *Cell Rep.* **3**, 342–349 (2013).
19. T. Matsuda, T. Yamamoto, A. Muraguchi, F. Saatcioglu, Cross-talk between transforming growth factor-β and estrogen receptor signaling through Smad3. *J. Biol. Chem.* **276**, 42908–42914 (2001).
20. S. Nagarajan, T. Hossan, M. Alawi, Z. Najafova, D. Indenbirken, U. Bedi, H. Taipaleenmaki, I. Ben-Batalla, M. Scheller, S. Loges, S. Knapp, E. Hesse, C. M. Chiang, A. Grundhoff, S. A. Johnsen, Bromodomain protein BRD4 is required for estrogen receptor-dependent enhancer activation and gene transcription. *Cell Rep.* **8**, 460–469 (2014).
21. R. C. Rao, Y. Dou, Hijacked in cancer: The KMT2 (MLL) family of methyltransferases. *Nat. Rev. Cancer* **15**, 334–346 (2015).
22. D. J. Steger, M. I. Lefterova, L. Ying, A. J. Stonestrom, M. Schupp, D. Zhuo, A. L. Vakoc, J. E. Kim, J. Chen, M. A. Lazar, G. A. Blobel, C. R. Vakoc, DOT1L/KMT4 recruitment and H3K79 methylation are ubiquitously coupled with gene transcription in mammalian cells. *Mol. Cell. Biol.* **28**, 2825–2839 (2008).
23. L. Cicatiello, M. Mutarelli, O. M. Grober, O. Paris, L. Ferraro, M. Ravo, R. Tarallo, S. Luo, G. P. Schroth, M. Seifert, C. Zinser, M. L. Chiusano, A. Traini, M. De Bortoli, A. Weisz, Estrogen receptor alpha controls a gene network in luminal-like breast cancer cells comprising multiple transcription factors and microRNAs. *Am. J. Pathol.* **176**, 2113–2130 (2010).
24. L. Zhang, L. Deng, F. Chen, Y. Yao, B. Wu, L. Wei, Q. Mo, Y. Song, Inhibition of histone H3K79 methylation selectively inhibits proliferation, self-renewal and metastatic potential of breast cancer. *Oncotarget* **5**, 10665–10677 (2014).
25. V. Härmä, H.-P. Schukov, A. Happonen, I. Ahonen, J. Virtanen, H. Siitari, M. Åkerfelt, J. Lötjönen, M. Nees, Quantification of dynamic morphological drug responses in 3D organotypic cell cultures by automated image analysis. *PLOS ONE* **9**, e96426 (2014).

26. A. Hurtado, K. A. Holmes, C. S. Ross-Innes, D. Schmidt, J. S. Carroll, FOXA1 is a key determinant of estrogen receptor function and endocrine response. *Nat. Genet.* **43**, 27–33 (2011).
27. V. Theodorou, R. Stark, S. Menon, J. S. Carroll, GATA3 acts upstream of FOXA1 in mediating ESR1 binding by shaping enhancer accessibility. *Genome Res.* **23**, 12–22 (2013).
28. H. Zeng, W. Xu, Ctr9, a key subunit of PAFc, affects global estrogen signaling and drives ERα-positive breast tumorigenesis. *Genes Dev.* **29**, 2153–2167 (2015).
29. W. Li, D. Notani, Q. Ma, B. Tanasa, E. Nunez, A. Y. Chen, D. Merkurjev, J. Zhang, K. Ohgi, X. Song, S. Oh, H.-S. Kim, C. K. Glass, M. G. Rosenfeld, Functional roles of enhancer RNAs for oestrogen-dependent transcriptional activation. *Nature* **498**, 516–520 (2013).
30. E. M. Stein, G. Garcia-Manero, D. A. Rizzieri, R. Tibes, J. G. Berdeja, M. R. Savona, M. Jongen-Lavrenic, J. K. Altman, B. Thomson, S. J. Blakemore, S. R. Daigle, N. J. Waters, A. B. Suttle, A. Clawson, R. Pollock, A. Krivtsov, S. A. Armstrong, J. DiMartino, E. Hedrick, B. Löwenberg, M. S. Tallman, The DOT1L inhibitor pinometostat reduces H3K79 methylation and has modest clinical activity in adult acute leukemia. *Blood* **131**, 2661–2669 (2018).
31. C. T. Campbell, J. N. Haladyna, D. A. Drubin, T. M. Thomson, M. J. Maria, T. Yamauchi, N. J. Waters, E. J. Olhava, R. M. Pollock, J. J. Smith, R. A. Copeland, S. J. Blakemore, K. M. Bernt, S. R. Daigle, Mechanisms of Pinometostat (EPZ-5676) Treatment-Emergent Resistance in *MLL*-Rearranged Leukemia. *Mol. Cancer Ther.* **16**, 1669–1679 (2017).
32. W. Yu, E. J. Chory, A. K. Wernimont, W. Tempel, A. Scopton, A. Federation, J. J. Marineau, J. Qi, D. Barsyte-Lovejoy, J. Yi, R. Marcellus, R. E. Iacob, J. R. Engen, C. Griffin, A. Aman, E. Wienholds, F. Li, J. Pineda, G. Estiu, T. Shatseva, T. Hajian, R. Al-Awar, J. E. Dick, M. Vedadi, P. J. Brown, C. H. Arrowsmith, J. E. Bradner, M. Schapira, Catalytic site remodelling of the DOT1L methyltransferase by selective inhibitors. *Nat. Commun.* **3**, 1288 (2012).
33. N. Brünner, T. L. Frandsen, C. Holst-Hansen, M. Bei, E. W. Thompson, A. E. Wakeling, M. E. Lippman, R. Clarke, MCF7/LCC2: A 4-hydroxytamoxifen resistant human breast cancer variant that retains sensitivity to the steroidal antiestrogen ICI 182,780. *Cancer Res.* **53**, 3229–3232 (1993).
34. S. Kangaspeska, S. Hultsch, A. Jaiswal, H. Edgren, J.-P. Mpindi, S. Eldfors, O. Brück, T. Aittokallio, O. Kallioniemi, Systematic drug screening reveals specific vulnerabilities and co-resistance patterns in endocrine-resistant breast cancer. *BMC Cancer* **16**, 378 (2016).
35. A. E. Lykkesfeldt, S. S. Larsen, P. Briand, Human breast cancer cell lines resistant to pure anti-estrogens are sensitive to tamoxifen treatment. *Int. J. Cancer* **61**, 529–534 (1995).
36. C. Ambrosino, R. Tarallo, A. Bamundo, D. Cuomo, G. Franci, G. Nassa, O. Paris, M. Ravo, A. Giovane, N. Zambrano, T. Lepikhova, O. A. Jänne, M. Baumann, T. A. Nyman, L. Cicatiello, A. Weisz, Identification of a hormone-regulated dynamic nuclear actin network associated with estrogen receptor α in human breast cancer cell nuclei. *Mol. Cell. Proteomics* **9**, 1352–1367 (2010).
37. R. Tarallo, A. Bamundo, G. Nassa, E. Nola, O. Paris, C. Ambrosino, A. Facchiano, M. Baumann, T. A. Nyman, A. Weisz, Identification of proteins associated with ligand-activated estrogen receptor α in human breast cancer cell nuclei by tandem affinity purification and nano LC-MS/MS. *Proteomics* **11**, 172–179 (2011).
38. E. K. Papachristou, K. Kishore, A. N. Holding, K. Harvey, T. I. Roumeliotis, C. S. R. Chilamakuri, S. Omarjee, K. M. Chia, A. Swarbrick, E. Lim, F. Markowetz, M. Eldridge, R. Siersbaek, C. S. D'Santos, J. S. Carroll, A quantitative mass spectrometry-based approach to monitor the dynamics of endogenous chromatin-associated protein complexes. *Nat. Commun.* **9**, 2311 (2018).
39. K. M. Jozwik, I. Chernukhin, A. A. Serandour, S. Nagarajan, J. S. Carroll, FOXA1 directs H3K4 monomethylation at enhancers via recruitment of the methyltransferase MLL3. *Cell Rep.* **17**, 2715–2723 (2016).
40. J. Qi, L. Huo, Y. T. Zhu, Y.-J. Zhu, Absent, small or homeotic 2-like protein (ASH2L) enhances the transcription of the estrogen receptor α gene through GATA-binding protein 3 (GATA3). *J. Biol. Chem.* **289**, 31373–31381 (2014).
41. J. S. Carroll, C. A. Meyer, J. Song, W. Li, T. R. Geistlinger, J. Eeckhoute, A. S. Brodsky, E. K. Keeton, K. C. Fertuck, G. F. Hall, Q. Wang, S. Bekiranov, V. Sementchenko, E. A. Fox, P. A. Silver, T. R. Gingeras, X. S. Liu, M. Brown, Genome-wide analysis of estrogen receptor binding sites. *Nat. Genet.* **38**, 1289–1297 (2006).
42. T. Ito, S. Kamijo, H. Izumi, K. Kohno, J. Amano, K.-i. Ito, Alteration of Y-box binding protein-1 expression modifies the response to endocrine therapy in estrogen receptor-positive breast cancer. *Breast Cancer Res. Treat.* **133**, 145–159 (2012).
43. W.-W. Tsai, Z. Wang, T. T. Yiu, K. C. Akdemir, W. Xia, S. Winter, C.-Y. Tsai, X. Shi, D. Schwarzer, W. Plunkett, B. Aronow, O. Gozani, W. Fischle, M. C. Hung, D. J. Patel, M. C. Barton, TRIM24 links a non-canonical histone signature to breast cancer. *Nature* **468**, 927–932 (2010).
44. H. Mohammed, I. A. Russell, R. Stark, O. M. Rueda, T. E. Hickey, G. A. Tarulli, A. A. Serandour, S. N. Birrell, A. Bruna, A. Saadi, S. Menon, J. Hadfield, M. Pugh, G. V. Raj, G. D. Brown, C. D'Santos, J. L. Robinson, G. Silva, R. Launchbury, C. M. Perou, J. Stingl, C. Caldas, W. D. Tilley, J. S. Carroll, Progesterone receptor modulates ERα action in breast cancer. *Nature* **523**, 313–317 (2015).
45. Z. Mo, M. Liu, F. Yang, H. Luo, Z. Li, G. Tu, G. Yang, GPR30 as an initiator of tamoxifen resistance in hormone-dependent breast cancer. *Breast Cancer Res.* **15**, R114 (2013).
46. G. Giurato, G. Nassa, A. Salvati, E. Alexandrova, F. Rizzo, T. A. Nyman, A. Weisz, R. Tarallo, Quantitative mapping of RNA-mediated nuclear estrogen receptor β interactome in human breast cancer cells. *Sci. Data* **5**, 180031 (2018).
47. J. A. Vizcaíno, A. Csordas, N. del-Toro, J. A. Dianes, J. Griss, I. Lavidas, G. Mayer, Y. Perez-Riverol, F. Reisinger, T. Ternent, Q.-W. Xu, R. Wang, H. Hermjakob, 2016 update of the PRIDE database and its related tools. *Nucleic Acids Res.* **44**, D447–D456 (2016).
48. T. Gao, B. He, S. Liu, H. Zhu, K. Tan, J. Qian, EnhancerAtlas: A resource for enhancer annotation and analysis in 105 human cell/tissue types. *Bioinformatics* **32**, 3543–3551 (2016).
49. H. Chen, C. Li, X. Peng, Z. Zhou, J. N. Weinstein, Cancer Genome Atlas Research Network, H. Liang, A pan-cancer analysis of enhancer expression in nearly 9000 patient samples. *Cell* **173**, 386–399.e12 (2018).
50. J. Gao, B. A. Aksoy, U. Dogrusoz, G. Dresdner, B. Gross, S. O. Sumer, Y. Sun, A. Jacobsen, R. Sinha, E. Larsson, E. Cerami, C. Sander, N. Schultz, Integrative analysis of complex cancer genomics and clinical profiles using the cBioPortal. *Sci. Signal.* 6, pl1 (2013).
51. B. Győrffy, A. Lanczky, A. C. Eklund, C. Denkert, J. Budczies, Q. Li, Z. Szallasi, An online survival analysis tool to rapidly assess the effect of 22,277 genes on breast cancer prognosis using microarray data of 1,809 patients. *Breast Cancer Res. Treat.* **123**, 725–731 (2010).
52. M. J. Cowley, M. Pinese, K. S. Kassahn, N. Waddell, J. V. Pearson, S. M. Grimmond, A. V. Biankin, S. Hautaniemi, J. Wu, PINA v2.0: Mining interactome modules. *Nucleic Acids Res.* **40**, D862–D865 (2012).
53. R. K. Kalathur, J. P. Pinto, M. A. Hernandez-Prieto, R. S. Machado, D. Almeida, G. Chaurasia, M. E. Futschik, UniHI 7: An enhanced database for retrieval and interactive analysis of human molecular interaction networks. *Nucleic Acids Res.* **42**, D408–D414 (2014).
54. O. Gilan, E. Y. Lam, I. Becher, D. Lugo, E. Cannizzaro, G. Joberty, A. Ward, M. Wiese, C. Y. Fong, S. Ftouni, D. Tyler, K. Stanley, L. MacPherson, C.-F. Weng, Y.-C. Chan, M. Ghisi, D. Smil, C. Carpenter, P. Brown, N. Garton, M. E. Blewitt, A. J. Bannister, T. Kouzarides, B. J. P. Huntly, R. W. Johnstone, G. Drewes, S.-J. Dawson, C. H. Arrowsmith, P. Grandi, R. K. Prinjha, M. A. Dawson, Functional interdependence of BRD4 and DOT1L in MLL leukemia. *Nat. Struct. Mol. Biol.* **23**, 673–681 (2016).

Acknowledgments: We acknowledge ELIXIR-IIB (http://elixir-italy.org/), the Italian Node of the European ELIXIR infrastructure (https://elixir-europe.org/), for the computational power support provided and Genomix4Life Srl. Some of the results displayed in the manuscript are based on data generated by the TCGA Research Network: http://cancergenome.nih.gov/. **Funding:** This work was supported by the Italian Association for Cancer Research (grant IG-17426), the Italian Ministry of Instruction and Research (Flagship Projects EPIGEN and InterOmics), and the University of Salerno (Fondi FARB 2017). **Author contributions:** G.N., R.T., G.G., and A.W. participated in the conception and design of the study. A. Salvati, R.T., V.G., E.A., A. Sellitto, and F.R. performed the in vitro experimental work and sequencing. D. Malanga, T.M., and E.M. performed the in vivo experimental work. T.A.N. and G.N. performed the proteomics analyses. G.G. and D. Memoli performed the statistical and bioinformatics analyses. A. Salvati, M.N., and M.Å. performed the 3D culture tests. S.K. generated and provided tamoxifen-resistant cell lines. G.N., A. Salvati, R.T., G.G., L.M., and A.W. coordinated and finalized the figure preparation, manuscript drafting, and revision. All authors read and approved the final manuscript. **Competing interests:** The authors declare that they have no competing interests. **Data and materials availability:** All data and accession numbers needed to evaluate the conclusions in the paper are present in the paper or the Supplementary Materials. Additional data related to this paper may be requested from the authors.

Submitted 27 September 2018
Accepted 21 December 2018
Published 6 February 2019
10.1126/sciadv.aav5590

Citation: G. Nassa, A. Salvati, R. Tarallo, V. Gigantino, E. Alexandrova, D. Memoli, A. Sellitto, F. Rizzo, D. Malanga, T. Mirante, E. Morelli, M. Nees, M. Åkerfelt, S. Kangaspeska, T. A. Nyman, L. Milanesi, G. Giurato, A. Weisz, Inhibition of histone methyltransferase DOT1L silences ERα gene and blocks proliferation of antiestrogen-resistant breast cancer cells. *Sci. Adv.* **5**, eaav5590 (2019).

Science Advances

Inhibition of histone methyltransferase DOT1L silences ERα gene and blocks proliferation of antiestrogen-resistant breast cancer cells

Giovanni Nassa, Annamaria Salvati, Roberta Tarallo, Valerio Gigantino, Elena Alexandrova, Domenico Memoli, Assunta Sellitto, Francesca Rizzo, Donatella Malanga, Teresa Mirante, Eugenio Morelli, Matthias Nees, Malin Åkerfelt, Sara Kangaspeska, Tuula A. Nyman, Luciano Milanesi, Giorgio Giurato and Alessandro Weisz

Sci Adv **5** (2), eaav5590.
DOI: 10.1126/sciadv.aav5590